

# Observation of antiphase dynamics of spatiotemporal chaos in a broad-area semiconductor laser

Masaya Arahata and Atsushi Uchida

Department of Information and Computer Sciences, Saitama University  
255 Shimo-Okubo Sakura-ku, Saitama City, Saitama 338-8570, Japan  
Emails: s13dm002@mail.saitama-u.ac.jp, auchida@mail.saitama-u.ac.jp

**Abstract**—We experimentally investigate spatio-temporal phase dynamics of a broad-area semiconductor laser. We observe in the experiment that the near-field pattern is constituted of several intensity peaks. We spatially isolate them one by one by using a slit as partial intensities. We measure the temporal waveform and frequency spectra of each partial intensity, and we also measure the intensity of the whole near-field pattern as a total intensity. We sum the corresponding spectral powers for each frequency component of each spectrum of the partial intensities. We compare this value to the spectral power corresponding to the same frequency in the total intensity. At some components in the frequency spectrum, the frequency peak of the total intensity is lower than the sum of those of the partial intensity, which suggests the existence of antiphase dynamics between the partial intensities. We find that inphase dynamics is observed at low frequency components. On the contrary, antiphase dynamics is observed for higher frequency component.

## 1. Introduction

Semiconductor lasers have been used for applications of laser processing and laser display, and high-power semiconductor lasers are required. However, there is a limitation of restricting output power to prevent catastrophic optical damage (COD) of the laser facet. A method of overcoming COD is to broaden the active region spatially, which is known as broad-area semiconductor lasers [1], [2]. Broad-area semiconductor lasers emit watt class of optical output power. However they have drawbacks that exhibit complex spatio-temporal dynamics of the laser output in the active region so called filamentation [3]-[6] (e.g. optical diffraction and carrier diffusion), which result from spatial hole-burning of the carrier density. Spatio-temporal irregular pulsations of the laser output have been reported at frequencies over 10 GHz [3], [6]. In addition, time-delayed optical feedback in semiconductor lasers leads to high-dimensional chaos [7]. These instabilities could be useful for implementation of fast physical random number generators based on chaotic dynamics [7]-[11]. Spatially-resolved output of broad-area semiconductor lasers could be used for parallel entropy sources for random number generators. However, phase relationship among the partial-

intensities may lead to a degradation of the randomness of the generated random numbers.

Antiphase dynamics of modal-intensity oscillations has been investigated intensively in multi-longitudinal-mode semiconductor lasers [12]-[15] and microchip solid-state lasers [16]-[19]. Note that antiphase dynamics is a property related to the coherence between the phases of the oscillations of the modal intensities rather than the optical phases. Chaotic temporal oscillations are too complex to determine the phase relationship. Thus inphase and antiphase dynamics of the chaotic oscillations are distinguished by comparing the radio-frequency (RF) spectra of the total intensity with the sum of modal intensities instead of the temporal waveforms[12]. Antiphase dynamics of multi-longitudinal modes has been observed for frequency components lower than the relaxation oscillation frequency of the laser. The low frequency components of modal intensities are cancelled out as antiphase dynamics, whereas the relaxation oscillation frequency components are coherently overlapped as inphase oscillations. These dynamics has been clearly explained in both experiments and numerical simulations [12]-[19]. However, no study on phase dynamics has been reported in broad-area semiconductor lasers. The investigation of inphase and antiphase dynamics in broad-area semiconductor lasers is required for understanding complex spatio-temporal dynamics, as well as for applications in fast physical random-number generators.

In this study, we experimentally investigate inphase and antiphase dynamics of spatially-resolved light intensities in a broad-area semiconductor laser. We measure the RF spectra of total and partial intensities to determine the phase relationship.

## 2. Experimental Setup

Figure 1 shows our experimental setup for the observation of the dynamics of the broad-area semiconductor laser. We use a broad-area semiconductor laser with 50- $\mu\text{m}$ -width active region. The optical wavelength of the laser is 808 nm. The injection current for the lasing threshold  $I_{th}$  is 160 mA. The output beam from the broad-area semiconductor laser is collimated with an aspheric lens and a cylindrical lens. The collimated beam is divided by a beam

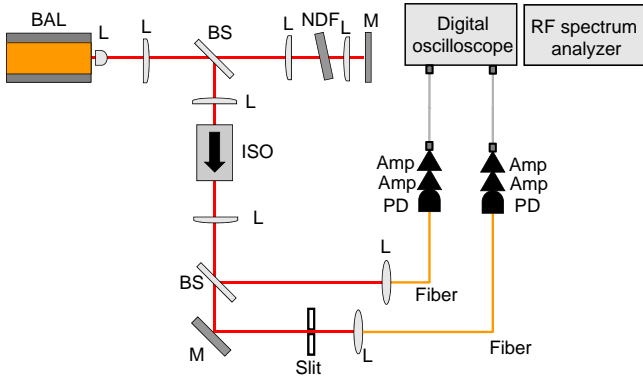


Figure 1: Experimental setup for the observation of phase dynamics in the broad-area semiconductor laser. Amp, electrical amplifier; BAL, broad-area semiconductor laser; BS, beam splitter; Fiber, optical fiber; ISO, optical isolator; L, lens; M, mirror; NDF, neutral density filter; PD, photodetector; Slit, variable slit.

splitter. One of the beams is reflected from an external mirror and fed back to the laser to generate chaotic oscillation of the laser output [2],[7]. The external cavity length is 51 cm, corresponding to the external-cavity frequency of 294 MHz. The optical feedback strength is adjusted by a neutral density filter. The other beam is divided into two beams, and one of them is used to observe temporal dynamics of the total laser intensity through an objective lens in front of an optical fiber. The other beam is used to observe one of the spatially-resolved partial intensities by using a slit and another objective lens in front of an optical fiber. A beam profiler is inserted to observe the near-field pattern and one of the partial intensities is selected by using the slit. The light beam focused on the lens of the optical fiber is converted to an electrical signal by using a photodetector and amplified by using two electrical amplifiers. The electrical signal is transmitted to a digital oscilloscope and a radio-frequency (RF) spectrum analyzer to observe temporal dynamics and RF spectra, respectively.

### 3. Experimental Results

#### 3.1. Near-field pattern and temporal dynamics

Figure 2 shows an example of the near-field pattern of the output of the broad-area semiconductor laser with optical feedback. The horizontal axis indicates beam position and the vertical axis indicates light intensity. In Fig. 2, the near-field pattern consists of several peaks at the injection current of  $1.31I_{th}$ .

We consider a situation where a chaotic output of the broad-area semiconductor laser can be used for parallel fast physical generation of random numbers. The near-field pattern is thus resolved by using a slit at the peak of the light intensities in Fig. 2. We investigate the phase dynam-

ics among these spatially-resolved light intensities for the application of parallel random number generators. Both the temporal waveforms and the RF spectra are observed for each partial intensity and for the total intensity.

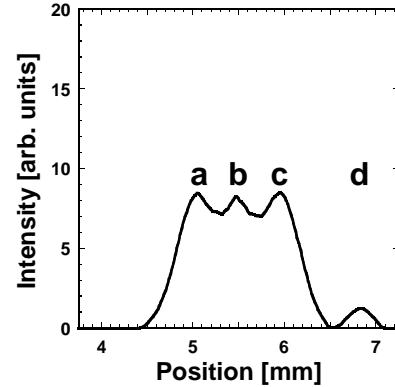


Figure 2: Near-field patterns of the broad-area semiconductor laser for the injection currents of  $1.31I_{th}$ .  $I_{th}$  is the injection current at the lasing threshold of the laser ( $I_{th} = 160$  mA). Each peak is spatially resolved by using a slit.

Figure 3(a) shows the chaotic temporal waveforms of the total intensity and the spatially-resolved partial intensities at the low injection current of  $1.31I_{th}$ . The upper and lower traces correspond to the temporal waveforms of the total and one of the partial intensities, respectively. The temporal waveform of the partial intensities includes both fast ( $\sim 6$  GHz) and slow ( $\sim 1$  GHz) fluctuations. However, the total intensity shows slow fluctuation mainly. Figure 3(b) shows the RF spectra of the total and one of the partial intensities, corresponding to Fig. 3(a). Note that the two RF spectra are shifted to the vertical direction for clarity, and the dotted lines indicate  $-70$  dBm. The peaks of the total intensity (black curve) are higher than those of the partial intensity (red curve) at around  $0.6$  GHz. On the contrary, the peaks of the partial intensity are higher than those of the total intensity at  $6.2$  GHz. We speculate that the fast frequency components are cancelled out due to antiphase dynamics, since the fast fluctuation observed in the partial intensity almost disappears in the temporal waveform of the total intensity in Fig. 3(a). The phase dynamics is thus dependent on the frequency of the chaotic oscillation.

#### 3.2. Quantitative estimation of inphase and antiphase dynamics from RF spectra

We use a method to determine inphase and antiphase dynamics of the spatially-resolved partial intensities from the comparison of RF spectra of the total intensity and sum of the partial intensities [12], since it is not easy to determine inphase and antiphase dynamics from chaotic temporal waveforms. In experiment, the RF spectrum of each partial intensity is observed. The spectral density of the  $i$ -th partial intensity at the frequency component  $f$  is rep-

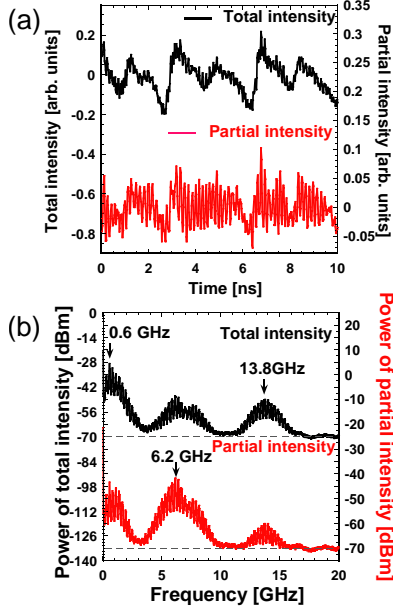


Figure 3: (a) Temporal waveforms and (b) corresponding RF spectra of the total intensity and one of the partial intensities at the injection current of  $1.31 I_{th}$ . The two RF spectra are shifted to the vertical direction for clarity, and the dotted lines indicate  $-70\text{dBm}$ .

represented as  $P_i(f)$  ( $i = 1, 2, \dots, n$  for a  $n$ -mode laser). The RF spectra of all the partial intensities are added at each frequency component in the linear scale, and the sum of the partial intensities  $P_{sum}(f)$  is obtained by  $P_{sum}(f) = \sum P_i(f)$  [17]. In addition, the RF spectrum of the total intensity is observed in experiment, denoted as  $P_{total}(f)$ . The value of  $P_{total}(f)$  is compared with that of  $P_{sum}(f)$  to determine the inphase and antiphase dynamics. Inphase dynamics is observed for  $P_{total}(f) > P_{sum}(f)$ . On the other hand, antiphase dynamics is observed for  $P_{total}(f) < P_{sum}(f)$ .

Constructive interference occurs among the partial intensities for inphase dynamics and  $P_{total}(f) > P_{sum}(f)$  is satisfied. On the contrary, destructive interference is observed among the partial intensities for antiphase dynamics and  $P_{total}(f) < P_{sum}(f)$  is satisfied [12]. Therefore, one can determine inphase or antiphase dynamics from the relationship between  $P_{total}(f)$  and  $P_{sum}(f)$ .

Figure 4(a) shows the RF spectra of the total intensity and the sum of the RF spectra of the partial intensities at the injection current of  $1.31I_{th}$ . The RF spectrum of the total intensity is higher than that of the sum of the partial intensities at the frequency region represented by the peak of 0.6 GHz, which includes the relaxation oscillation frequency. On the other hand, the RF spectrum of the total intensity is lower than the one of the sum of the partial intensities at the frequency region represented by the peak of 6.2 GHz.

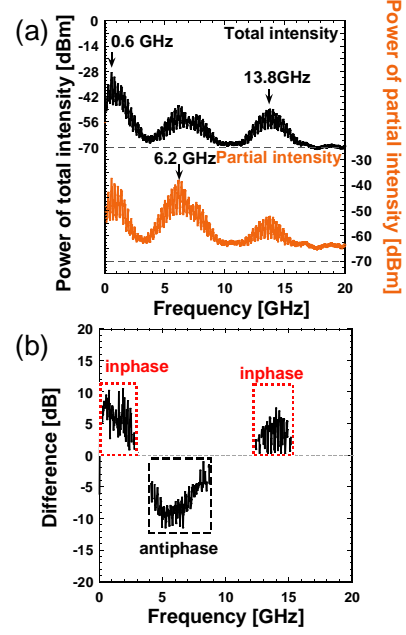


Figure 4: (a) RF spectra of the total intensity  $P_{total}(f)$  (upper) and the sum of the partial intensities  $P_{sum}(f)$  (lower) at the injection current of  $1.31I_{th}$ . The two RF spectra are shifted to the vertical direction for clarity, and the dotted lines indicate  $-70\text{ dBm}$ . (b) Difference in the two RF spectra  $\Delta P(f) = P_{total}(f) - P_{sum}(f)$ . Inphase and antiphase dynamics can be determined by  $\Delta P(f) > 0$  and  $\Delta P(f) < 0$ , respectively. Red and black dotted squares indicate the regions of inphase and antiphase dynamics, respectively.

We calculate the difference between the two RF spectra in Fig. 4(a),  $\Delta P(f) = P_{total}(f) - P_{sum}(f)$ . Inphase and antiphase dynamics can be determined by  $\Delta P(f) > 0$  and  $\Delta P(f) < 0$ , respectively. Here we defined the noise level of the RF spectrum less than  $-60\text{ dBm}$ , and we did not calculate the frequency components below the noise level to avoid the artifact of the calculation.

Figure 4(b) shows  $\Delta P(f)$  obtained from Fig. 4(a). It is found that inphase dynamics is observed at the low frequency region from 0.0 to 2.9 GHz, including the relaxation oscillation frequency. On the contrary, antiphase dynamics is observed in intermediate frequency region from 3.9 to 8.8 GHz. Inphase dynamics is also observed in high frequency region from 12.2 GHz to 15.3 GHz. Therefore, inphase and antiphase dynamics at particular frequency components can be clearly distinguished on the RF spectra.

The observation of inphase dynamics at low frequency component and antiphase dynamics at higher frequency component agrees well with the observation of the temporal waveforms shown in Fig. 3(a).

#### 4. Conclusions

We experimentally investigated the frequency dependence of inphase and antiphase dynamics among spatially-resolved light intensities in a chaotic broad-area semiconductor laser. We resolved partial intensities from the near-field pattern, and observed the temporal waveforms and the corresponding RF spectra. We compared the total intensity with the sum of the partial intensities on the RF spectra. In-phase dynamics is observed at both low and high frequency components, the relaxation oscillation frequency being included in the low frequency components. On the contrary, antiphase dynamics is observed at intermediate frequency components.

The investigation of the phase dynamics in chaotic broad-area semiconductor lasers could be useful for the application of fast physical random-number generators implemented in parallel.

#### Acknowledgments

We would like to thank Prof. Junji Ohtsubo and Prof. Takehiro Fukushima for their fruitful comments.

#### References

- [1] G. P. Agrawal, "Semiconductor lasers," 2nd ed., *Van Nostrand Reinhold, New York*, 1993.
- [2] J. Ohtsubo, "Semiconductor lasers: Stability, Instability and Chaos," 3rd ed., *Springer-Verlag, Berlin*, 1993.
- [3] T. Tachikawa, S. Takimoto, R. Shogenji, and J. Ohtsubo, "Dynamics of broad-area semiconductor lasers with short optical feedback," *IEEE Journal of Quantum Electron.*, vol.46, pp.140–149, 2010.
- [4] A. Takeda, R. Shogenji, and J. Ohtsubo, "Spatial-mode analysis in broad-area semiconductor lasers subjected to optical feedback," *Optical Review*, vol.20, pp.308–313, 2013.
- [5] O. Hess, and T. Kuhn, "Maxwell-bloch equations for spatially inhomogeneous semiconductor lasers. II. spatiotemporal dynamics," *Phys. Rev. A*, vol.54, pp.3360–3368, 1996.
- [6] I. Fischer, O. Hess, W. Elsässer and E. Gobel, "Complex spatio-temporal dynamics in the near-field of a broad-area semiconductor laser," *Eur. Phys. Lett.*, vol.35, pp.579–584, 1996.
- [7] A. Uchida, "Optical Communication with Chaotic Lasers, Applications of Nonlinear Dynamics and Synchronization," *Wiley-VCH, Weinheim, Germany*, 2012.
- [8] A. Uchida et al., "Fast physical random bit generation with chaotic semiconductor lasers," *Nature Photon.*, vol.2, pp.728–732, 2008.
- [9] X. -Z. Li, and S. -C. Chan, "Heterodyne random bit generation using an optically injected semiconductor laser in chaos," *IEEE J. Quantum Electron.*, vol.49, pp.829–838, 2013.
- [10] N. Oliver, M. C. Soriano, D. W. Sukow and I. Fischer, "Fast random bit generation using a chaotic laser: Approaching the information theoretic limit," *IEEE J. Quantum Electron.*, vol.49, pp.910–918, 2013.
- [11] T. Yamazaki, and A. Uchida, "Performance of random number generators using noise based superluminescent diode and chaos-based semiconductor lasers," *IEEE J. Sel. Topics Quantum Electron.*, vol.19, pp.0600309-1–0600309-9, 2013.
- [12] A. Uchida, Y. Liu, I. Fischer, P. Davis and T. Aida, "Chaotic antiphase dynamics and synchronization in multimode semiconductor lasers," *Phys. Rev. A*, vol.64, pp.023801, 2001.
- [13] I. V. Koryukin, and P. Mandel, "Antiphase dynamics of selectively coupled multimode semiconductor lasers," *IEEE J. Quantum Electron.*, vol.39, pp.1521–1525, 2003.
- [14] I. V. Koryukin, and P. Mandel, "Dynamics of semiconductor lasers with optical feedback: Comparison of multimode models in the low frequency fluctuation regime," *Phys. Rev. A*, vol.70, pp.053819, 2004.
- [15] C. Masoller, M. S. Torre and P. Mandel, "Antiphase dynamics in multimode semiconductor lasers with optical feedback," *Phys. Rev. A*, vol.71, pp.013818, 2005.
- [16] K. Otsuka, M. Georgiou and P. Mandel, "Intensity fluctuations in multimode lasers with spatial hole burning," *Jpn. J. Appl. Phys.*, vol.31, pp.L1250–L1252, 1992.
- [17] K. Otsuka, "Transverse effect on antiphase laser dynamics," *Jpn. J. Appl. Phys.*, vol.32, pp.L1414–L1417, 1993.
- [18] K. Otsuka, "Nonlinear Dynamics in Optical Complex Systems," *KTK Scientific, Tokyo, Japan*, 2000.
- [19] P. Mandel, "Theoretical Problems in Cavity Nonlinear Optics," *Cambridge Univ. Press, Cambridge, U.K.*, 1997.